

The gluon and charm content of the deuteron

Stanley J. Brodsky^a, Kelly Yu-Ju Chiu^a, Jean-Philippe Lansberg^b, Nodoka Yamanaka^{b,c}

^aSLAC National Accelerator Laboratory, Stanford University, Stanford, CA 94309, USA

^bIPNO, CNRS-IN2P3, Univ. Paris-Sud, Université Paris-Saclay, 91406 Orsay Cedex, France

^ciTHES Research Group, RIKEN, Wako, Saitama 351-0198, Japan

Abstract

We evaluate the frame-independent gluon and charm parton-distribution functions (PDFs) of the deuteron utilizing light-front quantization and the impulse approximation. We use a nuclear wave function obtained from solving the nonrelativistic Schrödinger equation with the realistic Argonne v18 nuclear force, which we fold with the proton PDF. The predicted gluon distribution in the deuteron (per nucleon) is a few percent smaller than that of the proton in the domain $x_{bj} = \frac{Q^2}{2p_N \cdot q} \sim 0.4$, whereas it is strongly enhanced for x_{bj} larger than 0.6. We discuss the applicability of our analysis and comment on how to extend it to the kinematic limit $x_{bj} \rightarrow 2$. We also analyze the charm distribution of the deuteron within the same approach by considering both the perturbatively and non-perturbatively generated (intrinsic) charm contributions. In particular, we note that the intrinsic-charm content in the deuteron will be enhanced due to 6-quark “hidden-color” QCD configurations.

1. Introduction

A primary challenge in nuclear physics is to study the structure and dynamics of nuclei from first principles in terms of the fundamental quark and gluon degrees of freedom of quantum chromodynamics (QCD). The conventional description of nuclear many-body systems, where nucleons are treated as elementary particles with phenomenological potentials, can be justified in the nonrelativistic domain [1–6]. However, in the short-distance, high-momentum-transfer region, quark and gluon fields play an essential role in describing nuclear systems, and non-nucleonic phenomena, such as QCD “hidden-color degrees” of freedom [7–10], become relevant. For example, the six-quark Fock state of the deuteron has five different SU(3) color-singlet contributions, only one of which projects to the standard proton and neutron three-quark clusters. The leading-twist shadowing [11–15] of nuclear parton distributions at small x_{bj} in the Gribov-Glauber theory is due to the destructive interference of two-step and one-step amplitudes, where the two-step amplitude depends on diffractive deep inelastic scattering (DDIS) $\ell N \rightarrow \ell' N' X$, leaving the struck nucleon intact. The study of the quark and gluon structure of nuclei thus illuminates the intersection between the nuclear and particle physics.

The quark and gluon distributions of nuclei also play an important role in high-energy astrophysics [16, 17]. An accurate knowledge of nuclear parton distributions is essential in many physics fields [18]. For example, the gluonic content of light nuclei is important in understanding the production of antiprotons in interstellar reactions. The charm-quark distribution function in nuclei at high x_{bj} can significantly change the predictions of the spectrum of cosmic neutrinos and is thus important to interpret the background of ultra-high-energy neutrinos which contribute to the IceCube experimental data [19, 20] in the high- x_F domain [21–

23]. Furthermore, the parton-distribution function (PDF) for nuclei is the initial condition controlling the dynamics of the possible formation and thermalization of the quark-gluon plasma (see *e.g.* [24]).

Collider experiments typically probe proton and nuclear PDFs in the region of small $x_{bj} = \frac{Q^2}{2p_N \cdot q}$ (see [25–28] for recent works showing the relevance of LHC heavy-flavor data to determine the gluon content of the nuclei at small x_{bj}). In contrast, fixed-target experiments can unveil the PDF over the full range of x_{bj} up to unity by taking advantage of the asymmetry of the experimental apparatus and the kinematics. New fixed-target experiments using the beams of the LHC are currently investigated (see the works of the AFTER@LHC study group [29–33]) following the very positive outcome of the data taking of the SMOG@LHCb system [34, 35]. In fixed-target experiments, one also has the advantage that the parton distributions of a large variety of nuclei, both polarized and unpolarized, can be measured. It is thus an important theoretical task to predict the gluon and heavy-quark distributions of nuclei.

We will focus on the deuteron, which is the simplest many-nucleon system, and thus can be evaluated with high accuracy in nuclear physics. It is therefore an excellent system where nuclear effects [7, 9, 36–60] can be studied. In addition, a careful study of the structure of the deuteron may provide accurate information on the quark and gluon structure of the neutron [61–63]. In particular, the gluon PDF of the neutron is of interest. The PDF of the deuteron near the maximal fraction $x_{bj} = 2$ (we use this definition in this work) can be constrained by perturbative QCD, since it is the dual of the deuteron form factor at high-momentum transfer Q^2 [64, 65]. In this work, we will mostly be interested in the region of $x_{bj} \sim 1$, a domain which AFTER@LHC can access.

As a first study, we have calculated the gluon PDF in the

deuteron within the impulse approximation which gives the leading contribution at $x_{bj} < 1$. To do so, we have solved the Schrödinger equation of the two-nucleon system with a phenomenological nuclear potential [1] using the Gaussian expansion method [66]. We have then derived the boost-invariant light-front wave function [67, 68] of the nucleus and convoluted it with the gluon distribution of the nucleon in order to obtain the gluon distribution of the deuteron. The complications of boosting an instant-form nucleon wavefunction to nonzero momentum are discussed in Ref. [69].

This paper is organized as follows. In the next section, we calculate the gluon PDF of the deuteron through the procedure mentioned above. In Section 3, we discuss the applicability of the impulse approximation and show our result. We also extend our discussion to illuminate the intrinsic heavy-quark contribution to the deuteron charm-quark distribution (Section 3.2). A summary is presented in the final section.

2. Derivation of the gluon PDF of the deuteron

2.1. Deuteron wave function

Let us now explain how we convolute the gluon PDF of the nucleon by the deuteron wave function in the impulse approximation [see Fig. 1 (a)]. The impulse approximation is the leading contribution in the chiral effective field theory (χ EFT) [48, 58]. We will show later that the two-nucleon contribution [Fig. 1 (b)] is subleading in the nucleon velocity expansion. These arguments lead us to consider a nonrelativistic framework.

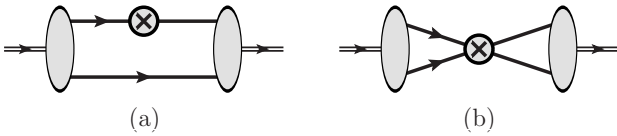


Figure 1: Schematic representation of the PDF of the deuteron. The solid and double lines denote the nucleon and the deuteron, respectively, and the cross indicates the PDF operator. There are two distinct contributions: (a) one-nucleon operator, working in the impulse approximation, (b) two-nucleon operator, relevant in high-momentum exchange.

We first calculate the wave function of the deuteron, given by the bound-state solution of the nonrelativistic two-nucleon Schrödinger equation with the Argonne v_{18} potential [1] as the nuclear force. To solve the equation, we use the Gaussian expansion method [66], where an accurate solution is provided as a superposition of Gaussians with geometric series of ranges. The Gaussian basis is given by

$$\Phi_{nlm}(\mathbf{r}) = N_{nl} r^l e^{-\nu_n r^2} Y_{lm}(\hat{r}), \quad (1)$$

where N_{nl} is the normalization constant of the Gaussian basis, \hat{r} the unit vector of the relative coordinate \mathbf{r} , and $\nu_n = \frac{1}{r_n^2} = \frac{1}{r_1 a^{n-1}}$ ($n = 1, \dots, n_{\max}$). We have taken $n_{\max} = 12$ Gaussians with $r_1 = 0.1$ fm and the common ratio a so that $r_{12} = 10$ fm. Note that the nuclear force has a strong tensor force which may change the orbital angular momentum

by two units, so the S -wave and D -wave states are relevant. The deuteron state is thus given by

$$|{}^2\text{H}, m_j\rangle = \sum_n c_n^{(s)} N_{n0} e^{-\nu_n r^2} Y_{00}(\hat{r}) \chi_{1, m_j} + \sum_{n'} c_{n'}^{(d)} N_{n'2} r^2 e^{-\nu_{n'} r^2} \sum_{m_l, m_s} f_{m_l m_s m_j} Y_{2 m_l}(\hat{r}) \chi_{1, m_s}, \quad (2)$$

where $\chi_{1, m_s} \equiv |s = 1, m_s\rangle$, and $f_{m_l m_s m_j} \equiv \langle l = 2, m_l, s = 1, m_s | j = 1, m_j\rangle$.

To solve the Schrödinger equation, we have to diagonalize the Hamiltonian matrix together with the nuclear norm matrix which involves the information of the overlap between Gaussian basis functions. This is a generalized eigenvalue problem (For details, see Section 2.1 of Ref. [66]). By diagonalizing the Hamiltonian, we obtain the wave function shown in Fig. 2, which has a dominant S -wave component and a D -wave component representing 6% of the total probability.

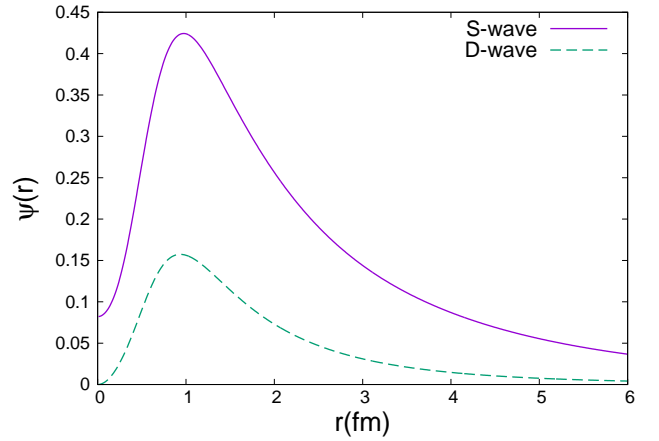


Figure 2: Radial component (spherical coordinate) of the deuteron wave function.

In our framework, the wave function is given as a superposition of Gaussians, so further transformations can analytically be performed. We then Fourier transform it and project the wave function onto the z -axis. After some manipulations, we obtain the following expression for the wave function of the unpolarized deuteron expressed in terms of the momentum in the z -axis p_z :

$$P(p_z) = \sum_n \sum_{n'} \frac{c_n^{(s)} c_{n'}^{(s)} N_{n0} N_{n'0} e^{-\frac{1}{4} \left(\frac{1}{\nu_n} - \frac{1}{\nu_{n'}} \right) p_z^2}}{8 \sqrt{\nu_n \nu_{n'}} (\nu_n + \nu_{n'})} + \sum_m \sum_{m'} \frac{c_m^{(d)} c_{m'}^{(d)} N_{m2} N_{m'2} e^{-\frac{1}{4} \left(\frac{1}{\nu_m} - \frac{1}{\nu_{m'}} \right) p_z^2}}{32 \sqrt{\nu_m \nu_{m'}} (\nu_m + \nu_{m'})} \times \left\{ \frac{8}{(\nu_m + \nu_{m'})^2} + \frac{2 p_z^2}{\nu_m \nu_{m'} (\nu_m + \nu_{m'})} + \frac{p_z^4}{4 \nu_m^2 \nu_{m'}^2} \right\} \quad (3)$$

Let us note that the cross-terms between $c_n^{(s)}$ and $c_{n'}^{(d)}$ cancel.

The corresponding probability distribution is shown in Fig. 3. The distribution of the nucleon momentum is centered at $p_z = 0$, and the standard deviation is close to 50 MeV. This is due to the kinetic energy of the nucleon (about 20 MeV), which is the bound-state effect of the nuclear force. Figure 3 also displays the contribution from the S -wave, which is nearly identical to the total result.

In Fig. 3, we also show the momentum distribution of the nucleon inside a typical heavy nucleus with the Fermi energy $\epsilon_F \equiv \frac{p_F^2}{2m_N} = 33$ MeV. The smearing of the momentum distribution is given by [43]

$$P(p_z) = \frac{1}{\sqrt{2\pi}\gamma_F} \exp\left(-\frac{p_z^2}{2\gamma_F}\right), \quad (4)$$

where $\gamma_F = \frac{1}{5}p_F^2$. One sees that the momentum distribution of the deuteron is narrower than that of a typical heavy nucleus.

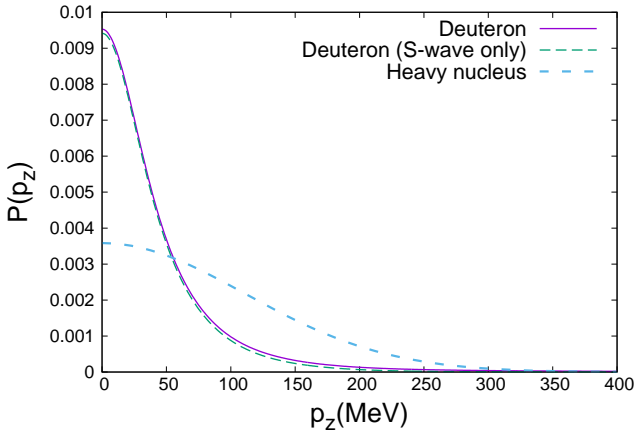


Figure 3: Momentum z -axis component of the deuteron wave function. The data for a typical nucleus with a Fermi energy $\epsilon_F = 33$ MeV are also shown for comparison (labeled as “Heavy nucleus”).

2.2. Light-front momentum fraction

We now calculate the light-front momentum distribution of the nucleon in the deuteron. Note that the procedure to obtain a wave function in the light-front frame from the instant-form is not unique. In this work, we follow the recipe of Ref. [70] (see also [43, 71–73]) giving the wave function in the light-front frame as

$$\psi(\mathbf{p}_\perp, z) = \sqrt{\frac{\partial p_z(\mathbf{p}_\perp, z)}{\partial z}} \psi(\mathbf{p}_\perp, p_z), \quad (5)$$

where $p_z = (z-1)\sqrt{\frac{m_N^2 + \mathbf{p}_\perp^2}{z(2-z)}}$. The momentum fraction of the nucleon in the deuteron z is defined in the interval $0 \leq z \leq 2$. This can consistently be derived using z defined by

$$z \equiv A \frac{p_N^+}{p_A^+} = \frac{A}{m_A} \left[\sqrt{m_N^2 + p_z^2 + \mathbf{p}_\perp^2} + p_z \right], \quad (6)$$

where p_N^+ and p_A^+ are the momentum of the nucleon and of the nucleus in the light-front frame, respectively, and A the nucleon number of the nucleus ($A = 2$ for the deuteron). We then have $z \leq A$. The masses of the nucleon and of the nucleus are labeled by m_N and m_A , respectively. By nonrelativistically reducing the nuclear binding effect ($p_z^2 + \mathbf{p}_\perp^2/m_N^2 \ll 1$ and $m_A \approx Am_N$, one obtains [43]

$$z - 1 \approx \frac{p_z}{m_N}. \quad (7)$$

This can however be improved by considering the shift of the energy by the moving nucleon inside the deuteron. The momentum fraction is then

$$z = A \frac{p_N^+}{p_A^+} \approx A \frac{E_N + p_z}{2E_N} = 1 + \frac{p_z}{E_N} = 1 + \frac{p_z}{\sqrt{p_z^2 + m_N^2}}, \quad (8)$$

where we still neglect \mathbf{p}_\perp . By solving the above equation in term of p_z , the nucleon longitudinal momentum inside the deuteron satisfies

$$p_z = \frac{z-1}{\sqrt{z(2-z)}} m_N. \quad (9)$$

We think this manipulation is more suitable for light-front dynamics than the approximation used in Ref. [43].

We then apply this variable change to the previously obtained z -axis momentum fraction $P(p_z) \equiv |\psi(p_z)|^2$. We have

$$N_{N/A}(z) dz = \frac{m_N}{\sqrt{z(2-z)^3}} \left| \psi \left[\frac{z-1}{\sqrt{z(2-z)}} m_N \right] \right|^2 dz. \quad (10)$$

This relation agrees with the recipe of Ref. [70].

This yields the light-front distribution plotted in Fig. 4, where one sees that the momentum fraction of the nucleon is broader in the deuteron than in a typical heavy nucleus, which is expected from the importance of the Fermi motion.

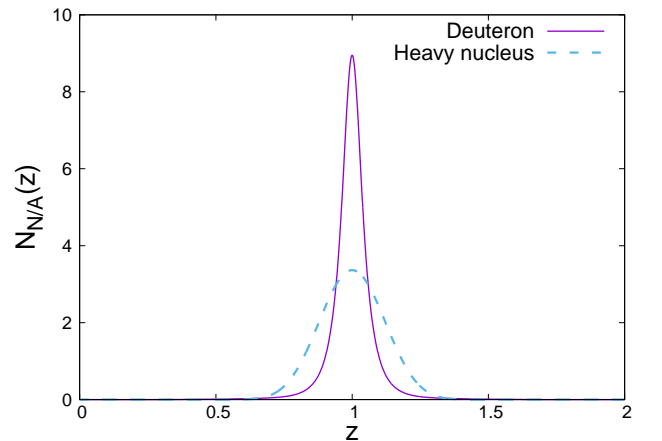


Figure 4: Momentum fraction of the nucleon in the deuteron. The data for a typical heavy nucleus with a Fermi energy $\epsilon_F = 33$ MeV are also shown for comparison (labeled as “Heavy nucleus”).

2.3. Gluon distribution

Now that we have the light-front distribution of the nucleon in the deuteron, we can derive the gluon PDF in the deuteron using the impulse approximation, by folding the gluon PDF of the nucleon [74–81] by $N_{N/A}(z)$. Since we are interested in the high- x behavior of the gluon PDF, we need a well behaved gluon PDF up to 1. For this reason, we prefer to use GRV98 [82].

The gluon PDF in the deuteron is obtained by folding the gluon PDF of the proton $G^p(x)$ by the light-front distribution of the nucleon inside the deuteron $N_{N/A}(z)$:

$$\begin{aligned} G^d(x, \mu_F) &= 2 \int dy dz N_{N/A}(z) G^p(y, \mu_F) \delta(yz - x) \\ &= 2 \int_x^A N_{N/A}(z) \frac{1}{z} G^p(x/z, \mu_F) dz, \end{aligned} \quad (11)$$

where μ_F is the factorization scale. We note that the effect of the scale evolution is contained in $G^p(x/z, \mu_F)$. This operation consists of calculating the contribution depicted by the diagram of Fig. 1 (a). In our computation, we of course assume that the proton and the neutron have the same gluon PDF, hence the factor of two in Eq. (11).

3. Results and discussion

3.1. Domain of applicability

Before plotting our results, let us discuss the domain of applicability of our calculation. Indeed, we assumed that the nucleon inside the deuteron is not modified from the on-shell one. The nucleons in the deuteron can be considered almost on-shell when the invariant mass of the nucleon pair M_{pn} has a small virtuality compared to the binding of the deuteron:

$$M_{pn}^2 - m_d^2 < m_d \times \epsilon_d, \quad (12)$$

where m_d and ϵ_d are respectively the deuteron mass and binding energy. The above condition of virtuality can be converted to a constraint on the nucleon velocity, that is $v = \frac{p_z}{m_N}$ by using Eq. (9) [or Eq. (7)]. This gives $v < 0.004$ which is obviously nonrelativistic. From this inequality, we can then derive the corresponding region of the momentum fraction of the gluon in the deuteron, by computing the average $\langle z \rangle$ as a function of x . This yields a conservative limit, $0 < x < 0.7$, outside which the off-shell correction may be relevant.

Let us now inspect what such off-shell effects may be. We start by discussing the two-nucleon effects [see Fig. 1 (b)]. The n th moment of the PDF can indeed be expanded in terms of the velocity of the nucleus v_A as [48]

$$\langle x^n \rangle_{g|A} = v_{A,\mu_0} \cdots v_{A,\mu_n} \langle A | \mathcal{O}_g^{\mu_0 \cdots \mu_n} | A \rangle, \quad (13)$$

where $\mathcal{O}_g^{\mu_0 \cdots \mu_n}$ is the gluon density operator. We note that the nuclear velocity is equal to the nucleon velocity v , up to small x corrections due to the nuclear binding. On the other hand, $\langle x^n \rangle_{g|A}$ can be expressed in terms of the nonrelativistic nucleon operators as

$$\langle x^n \rangle_{g|A} = \langle x^n \rangle_g [A + \langle A | \alpha_n (N^\dagger N)^2 | A \rangle], \quad (14)$$

where $\langle x^n \rangle_g$ is the n th moment of the gluon PDF of the nucleon. The first term A is the nucleon number, obtained from the one-nucleon operator $\langle A | N^\dagger N | A \rangle = A$. The nuclear matrix element $\langle A | \alpha_n (N^\dagger N)^2 | A \rangle$ provides the nuclear modification effect, and depends on the renormalization scale but not on the momentum fraction. The coefficient α_n is proportional to the n th moment of the nuclear modification effect of the PDF, which is the residual piece of the nuclear PDF after subtracting the gluon PDF of free nucleons.

The zeroth moment α_0 is zero, due to charge conservation, and the first moment α_1 is known to be small from experiment [83]. At the hadron level, the leading off-shell correction is the pion exchange-current [48, 84, 85], but these contributions are N³LO in χ EFT, thus small. This means that the nuclear modification effect is expected to be small in the nonrelativistic regime. The first off-shell effect therefore starts from v^2 which means that the constraint discussed above, $v < 0.004$, is probably too conservative.

Let us now see the range of velocities in which our framework holds. In Fig. 5, we plot the averaged squared velocity of the nucleon as a function of the gluon momentum fraction x . We of course exclude the region $\langle v^2 \rangle > 1$ which is unphysical. We note that $\langle v^2 \rangle$ is still small at $x = 1.1$, $\langle v^2 \rangle \approx 0.3$ and therefore consider the domain of applicability of our framework as $0 < x < 1.1$, where the off-shell effects are likely small.

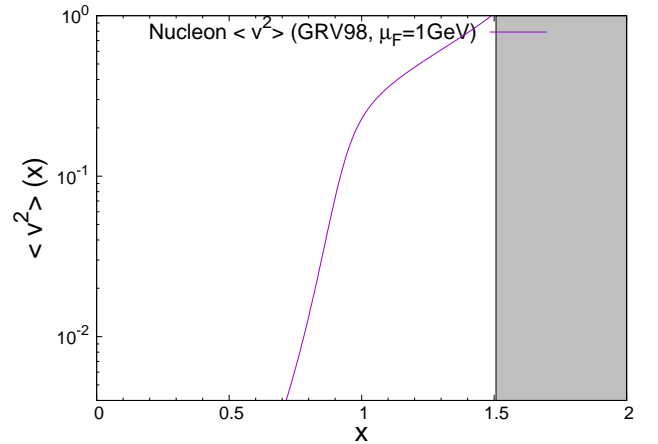


Figure 5: The velocity distribution of the nucleon in the deuteron ($\langle v^2 \rangle$) as a function of the gluon momentum fraction x obtained in our framework. The region where $\langle v^2 \rangle > 1$ is unphysical (grey band).

According to the above discussion, we will show the result of our calculation of the gluon PDF in the deuteron up to $x \approx 1.1$ in Fig. 6. The gluon PDF of the deuteron $G^d(x, \mu_F)$ shows a monotonic decrease. In the region $0 < x < 0.6$, $G^d(x, \mu_F) \approx 2G^p(x, \mu_F)$ within 5%, as expected. It is also notable that the ratio G^d/G^p is larger than unity for $0 < x < 0.2$, and that it shows a minimum near $x = 0.4$. Above $x \sim 0.6$, the ratio G^d/G^p grows rapidly due to the falloff of the PDF of the proton. This is due to the Fermi motion, where the momentum of the nucleon in the deuteron is pushed to the high momentum region, in a

similar way as the quark PDF.

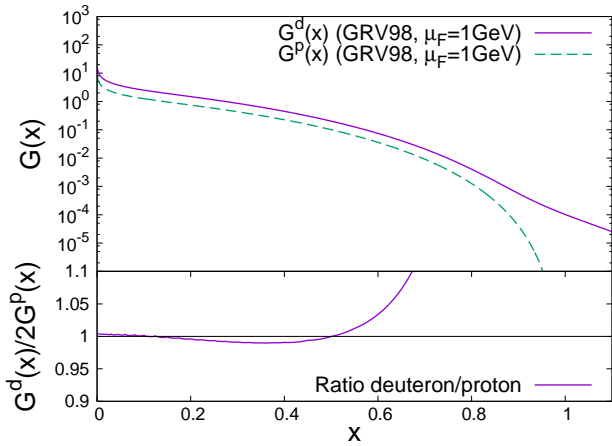


Figure 6: Gluon PDF in the deuteron and in the nucleon.

3.2. Charm distribution of the deuteron

Another interesting point to discuss is the charm-quark distribution, which can be analyzed in the same way as that of the gluon. The charm-quark distribution of the deuteron can equally be calculated in the domain of applicability of our framework discussed in Sec. 3.1 ($0 < x < 1.1$).

The charm quarks in a nucleon are virtually created by the gluon splitting (see Fig. 7) at leading order. The distribution of the charm quark generated by this subprocess inherits the gluon distribution, and decreases monotonically in x . We have calculated this contribution by using the charm PDF of CTEQ-JLAB 15 [86] which we fold with $N_{N/A}(z)$ discussed in Section 2.3. The result of our calculation is shown in Fig. 8. The behavior of the charm PDF of the deuteron due to the gluon splitting is similar to that of the gluon. The ratio of the charm PDFs of the deuteron (per nucleon) to the proton is unity within 5% for $x < 0.4$, and it deviates from unity for $x > 0.4$ due to Fermi motion, as expected from the impulse approximation.

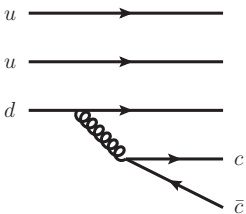


Figure 7: Diagrammatic representation of the charm-quark creation in a nucleon via gluon splitting.

The distribution of charm quarks in the nucleon however receives additional non-perturbative contributions from the charm quark-antiquark pair creation which are multi-connected by two or more gluons coupling to different va-

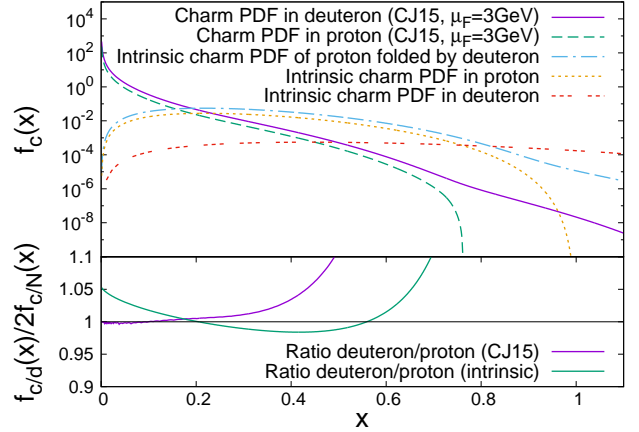


Figure 8: Charm PDF in the deuteron and in the nucleon.

lence quarks (see Fig. 9). This *intrinsic-charm* contribution, although suppressed since it is higher order in α_s , is favored by a higher probability due to the sharing of momenta from different valence quarks. This is in contrast to the gluon-splitting contributions where the charm and anti-charm quarks couples to a single valence quark. In the limit of heavy quarks (Q), the intrinsic heavy quark distribution in a hadron is suppressed as m_Q^{-2} , as can be derived by the application of the operator product expansion [87–89]. A model for the charm distribution in the nucleon based on kinematical constraints is given in Refs. [90, 91]

$$f_{c/N}^{\text{int}}(x) = 1800\mathcal{N}x^2 \left[\frac{1}{3}(1-x)(1+10x+x^2) + 2x(1+x)\ln x \right]. \quad (15)$$

The normalization \mathcal{N} is phenomenologically determined as $\mathcal{N} \sim 0.01$ [91]. This distribution peaks at $x \sim 0.2$, and becomes dominant for $x \gtrsim 0.2$

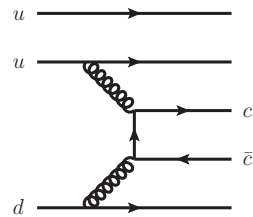


Figure 9: Diagrammatic representation of the intrinsic charm in a nucleon.

We plot in Fig. 8 the intrinsic-charm distribution of the deuteron calculated in our framework. As is the case of the gluon splitting, the Fermi motion alters the ratio of the deuteron PDFs (per nucleon) to that of the proton from unity for $x > 0.6$. We also observe that this ratio, although consistent with unity within 5%, varies more than that of the gluon PDFs in the region $0 < x < 0.6$.

We can also derive an intrinsic-charm distribution of the deuteron by considering a six-valence-parton configuration

(see Fig. 10). It can be calculated by rescaling the endpoint of Eq. (15) from $x = 1$ to $x = 2$. The normalization of the intrinsic-charm contribution to the deuteron is currently not known (we plot it in Fig. 8, with $\mathcal{N} = 10^{-4}$). There are however some arguments suggesting a sizable contribution of this contribution. Indeed, beside the argument of the momentum-fraction sharing by several valence particles enhancing the intrinsic-charm content at high x , there is another enhancement from the combinatoric factors in the deuteron case. For the gluon splitting, we obviously have a factor of 6, whereas for the intrinsic charm generated by the radiation of two gluons from two distinct quarks, we have a factor of 15 (see Fig. 10 (a)). The enhancement may even be larger for the intrinsic charm created by the three-gluon emission although it is even higher order in α_s , since we have a combinatoric factor of 20 (see Fig. 10 (b)). Note that this combinatoric enhancement is absent in the case of the nucleon. The intrinsic-charm contribution generated off three-gluon emission may also kinematically be more advantageous than the two-gluon case, since the momenta of valence quarks can stay closer to the valence configuration after the gluon radiation. It would thus be interesting to perform measurements sensitive to the charm content of the deuteron at $x \sim 1$. Fixed-target experiments at the LHC with the LHCb or ALICE detector provide an ideal setup for such measurements.

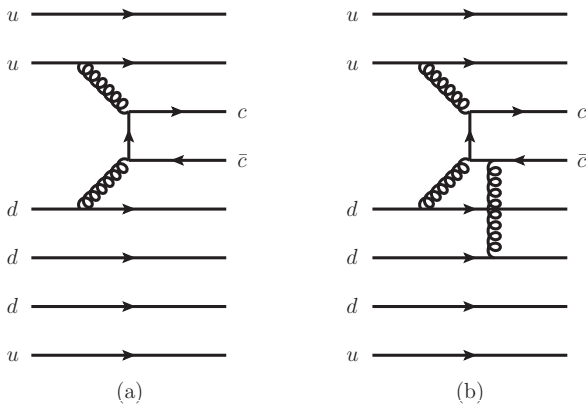


Figure 10: Diagrammatic representation of the intrinsic-charm generation in the deuteron: (a) from two-gluon fusion, (b) the α_s suppressed –but combinatoric enhanced– 3-gluon fusion.

4. Summary

In this work, we have calculated the gluon and charm PDFs of the deuteron in the light-front quantization. We used the impulse approximation where the input nuclear wave function is obtained by solving the nonrelativistic Schrödinger equation with the phenomenological Argonne v_{18} nuclear potential as input. Although we only analyzed the nonrelativistic regime, the range of applicability our computation is estimated to extend up to $x \sim 1.1$.

We have found that the gluon and charm PDFs of the deuteron (per nucleon) at low x only differs by a few percent from that of the proton, as expected for nonrelativistic nucleons in the nucleus. However as x becomes close to unity, their distributions deviate significantly from that of the nucleon due to Fermi motion. This should be taken into account when extracting the gluon PDF of the neutron via this system.

We also discussed the charm PDF of the deuteron, which is potentially very interesting at $x \sim 1$ due to the intrinsic-charm contribution. The intrinsic charm of the deuteron is enhanced by the combinatoric factors characteristic for gluon emission and the sharing of the momentum by valence partons, although the overall normalization is somewhat uncertain. We expect the charm distribution in the deuteron to be studied in the region $0 < x < 1.1$ by future experiments –particularly in future fixed-target experiments using the LHC beams– in order to determine the normalization of the intrinsic-charm and hidden-color states.

In the limit of high-momentum scale $Q^2 \rightarrow \infty$ for exclusive scatterings, other structures with the same quantum numbers as the $|NN\rangle$ state, such as the $\Delta\Delta$ states, or the *hidden-color configurations* [7–10], in which quarks are not arranged to form two color-singlet baryons, become relevant as Fock states. Indeed, in the short distance limit, 80% of the deuteron will be composed of hidden-color states. This state should be continuously related to the almost maximal $|NN\rangle$ state at low resolution via the renormalization group equation. The composition at intermediate momentum scales also involves higher Fock states with a valence gluon [92], such as $|(uudddg)\rangle$. We note that the composition at intermediate distances can only be calculated if the normalization of the Fock state at some scale is known, as is the case for the renormalization group equation analysis. As for now, the implication of these states for inclusive reactions at finite x (away from 2 in the deuteron case), and thus the PDFs, remains to be studied, and is beyond the scope of our exploratory study.

At the endpoint ($x \sim 2$), where only one gluon is carrying almost the entire momentum of the deuteron, the gluon PDF behavior is however related to the form factor of the system at short distances [36, 93, 94], and is known analytically. The counting rules indeed predict $G^d(x) \propto (2-x)^{11}$ [36, 68, 94, 95]. Since the partons are maximally virtual in this limit, the deuteron has to be expressed in terms of quarks and gluons, and it is therefore not possible to discuss with our framework. Extending our nonrelativistic results to this limiting case, is also left for a future work especially since it seems difficult experimentally accessible in a near future.

Our framework could be extended to the case of the gluon and charm PDF in heavier nuclei, such as the ${}^4\text{He}$, which is one of the main ingredient of the interstellar matter, and for ${}^{14}\text{N}$ and ${}^{16}\text{O}$, which are the main components of the atmosphere. Such analyses would be important to reduce the theoretical uncertainty of the cross section of the reactions between primary cosmic rays and the interstellar matter, as well as to predict the ultra-high-energy neutrino background

in terrestrial experiments such as IceCube [19–23]. A better knowledge of the gluon PDFs of light nuclei, *e.g.* ^3He and ^4H , is therefore crucial for high-energy astrophysics, and they could be measured in the near future in LHC fixed-target experiments.

Acknowledgements

We thank Jaume Carbonell and Cedric Lorcé for useful comments and suggestions. NY is supported by JSPS Postdoctoral Fellowships for Research Abroad and by the RIKEN iTHES Project. This work has been supported in part by the French CNRS via the IN2P3 project TMD@NLO and by the French ANR via the LABEX P2IO. S.J.B. is supported by the Department of Energy, contract DE-AC02-76SF00515. SLAC-PUB-17253.

References

- [1] R. B. Wiringa, V. G. J. Stoks, and R. Schiavilla, “An Accurate nucleon-nucleon potential with charge independence breaking,” *Phys. Rev. C* **51** (1995) 38–51, [arXiv:nucl-th/9408016 \[nucl-th\]](#).
- [2] U. van Kolck, “Few nucleon forces from chiral Lagrangians,” *Phys. Rev. C* **49** (1994) 2932–2941.
- [3] S. C. Pieper, V. R. Pandharipande, R. B. Wiringa, and J. Carlson, “Realistic models of pion exchange three nucleon interactions,” *Phys. Rev. C* **64** (2001) 014001, [arXiv:nucl-th/0102004 \[nucl-th\]](#).
- [4] H. Kamada *et al.*, “Benchmark test calculation of a four nucleon bound state,” *Phys. Rev. C* **64** (2001) 044001, [arXiv:nucl-th/0104057 \[nucl-th\]](#).
- [5] J. Carlson, S. Gandolfi, F. Pederiva, S. C. Pieper, R. Schiavilla, K. E. Schmidt, and R. B. Wiringa, “Quantum Monte Carlo methods for nuclear physics,” *Rev. Mod. Phys.* **87** (2015) 1067, [arXiv:1412.3081 \[nucl-th\]](#).
- [6] P. Reinert, H. Krebs, and E. Epelbaum, “Semilocal momentum-space regularized chiral two-nucleon potentials up to fifth order,” [arXiv:1711.08821 \[nucl-th\]](#).
- [7] S. J. Brodsky, C.-R. Ji, and G. P. Lepage, “Quantum Chromodynamic Predictions for the Deuteron Form-Factor,” *Phys. Rev. Lett.* **51** (1983) 83.
- [8] S. J. Brodsky and C.-R. Ji, “Evolution of Relativistic Multi - Quark Systems,” *Phys. Rev. D* **33** (1986) 1406.
- [9] S. J. Brodsky and C.-R. Ji, “Factorization Property of the Deuteron,” *Phys. Rev. D* **33** (1986) 2653.
- [10] M. Bashkanov, S. J. Brodsky, and H. Clement, “Novel Six-Quark Hidden-Color Dibaryon States in QCD,” *Phys. Lett. B* **727** (2013) 438–442, [arXiv:1308.6404 \[hep-ph\]](#).
- [11] A. H. Mueller and J.-w. Qiu, “Gluon Recombination and Shadowing at Small Values of x ,” *Nucl. Phys. B* **268** (1986) 427–452.
- [12] S. J. Brodsky and H. J. Lu, “Shadowing and Antishadowing of Nuclear Structure Functions,” *Phys. Rev. Lett.* **64** (1990) 1342.
- [13] G. Piller and W. Weise, “Nuclear deep inelastic lepton scattering and coherence phenomena,” *Phys. Rept.* **330** (2000) 1–94, [arXiv:hep-ph/9908230 \[hep-ph\]](#).
- [14] N. Armesto, “Nuclear shadowing,” *J. Phys. G* **32** (2006) R367–R394, [arXiv:hep-ph/0604108 \[hep-ph\]](#).
- [15] L. Frankfurt, V. Guzey, and M. Strikman, “Dynamical model of antishadowing of the nuclear gluon distribution,” *Phys. Rev. C* **95** no. 5, (2017) 055208, [arXiv:1612.08273 \[hep-ph\]](#).
- [16] R. Enberg, M. H. Reno, and I. Sarcevic, “Prompt neutrino fluxes from atmospheric charm,” *Phys. Rev. D* **78** (2008) 043005, [arXiv:0806.0418 \[hep-ph\]](#).
- [17] A. Bhattacharya, R. Enberg, M. H. Reno, I. Sarcevic, and A. Stasto, “Perturbative charm production and the prompt atmospheric neutrino flux in light of RHIC and LHC,” *JHEP* **06** (2015) 110, [arXiv:1502.01076 \[hep-ph\]](#).
- [18] M. Arneodo, “Nuclear effects in structure functions,” *Phys. Rept.* **240** (1994) 301–393.
- [19] IceCube Collaboration, M. G. Aartsen *et al.*, “Observation of High-Energy Astrophysical Neutrinos in Three Years of IceCube Data,” *Phys. Rev. Lett.* **113** (2014) 101101, [arXiv:1405.5303 \[astro-ph.HE\]](#).
- [20] IceCube Collaboration, M. G. Aartsen *et al.*, “Observation and Characterization of a Cosmic Muon Neutrino Flux from the Northern Hemisphere using six years of IceCube data,” *Astrophys. J.* **833** no. 1, (2016) 3, [arXiv:1607.08006 \[astro-ph.HE\]](#).
- [21] F. Halzen and L. Wille, “Charm contribution to the atmospheric neutrino flux,” *Phys. Rev. D* **94** no. 1, (2016) 014014, [arXiv:1605.01409 \[hep-ph\]](#).
- [22] R. Laha and S. J. Brodsky, “IceCube can constrain the intrinsic charm of the proton,” *Phys. Rev. D* **96** no. 12, (2017) 123002, [arXiv:1607.08240 \[hep-ph\]](#).
- [23] A. V. Giannini, V. P. Goncalves, and F. S. Navarra, “On the intrinsic charm contribution to the prompt atmospheric neutrino flux,” [arXiv:1803.01728 \[hep-ph\]](#).
- [24] A. Andronic *et al.*, “Heavy-flavour and quarkonium production in the LHC era: from proton-proton to heavy-ion collisions,” *Eur. Phys. J. C* **76** no. 3, (2016) 107, [arXiv:1506.03981 \[nucl-ex\]](#).
- [25] PROSA Collaboration, O. Zenaiev *et al.*, “Impact of heavy-flavour production cross sections measured by the LHCb experiment on parton distribution functions at low x ,” *Eur. Phys. J. C* **75** no. 8, (2015) 396, [arXiv:1503.04581 \[hep-ph\]](#).
- [26] R. Gauld and J. Rojo, “Precision determination of the small- x gluon from charm production at LHCb,” *Phys. Rev. Lett.* **118** no. 7, (2017) 072001, [arXiv:1610.09373 \[hep-ph\]](#).
- [27] A. Kusina, J.-P. Lansberg, I. Schienbein, and H.-S. Shao, “Gluon shadowing and antishadowing in heavy-flavor production at the LHC,” [arXiv:1712.07024 \[hep-ph\]](#).
- [28] J.-P. Lansberg and H.-S. Shao, “Towards an automated tool to evaluate the impact of the nuclear modification of the gluon density on quarkonium, D and B meson production in proton-nucleus collisions,” *Eur. Phys. J. C* **77** no. 1, (2017) 1, [arXiv:1610.05382 \[hep-ph\]](#).
- [29] S. J. Brodsky, F. Fleuret, C. Hadjidakis, and J. P. Lansberg, “Physics Opportunities of a Fixed-Target Experiment using the LHC Beams,” *Phys. Rept.* **522** (2013) 239–255, [arXiv:1202.6585 \[hep-ph\]](#).
- [30] B. Trzeciak, C. Da Silva, E. G. Ferreira, C. Hadjidakis, D. Kikola, J. P. Lansberg, L. Massacrier, J. Seixas, A. Uras, and Z. Yang, “Heavy-ion Physics at a Fixed-Target Experiment Using the LHC Proton and Lead Beams (AFTER@LHC): Feasibility Studies for Quarkonium and Drell-Yan Production,” *Few Body Syst.* **58** no. 5, (2017) 148, [arXiv:1703.03726 \[nucl-ex\]](#).
- [31] D. Kikola, M. G. Echevarria, C. Hadjidakis, J.-P. Lansberg, C. Lorce, L. Massacrier, C. M. Quintans, A. Signori, and B. Trzeciak, “Feasibility Studies for Single Transverse-Spin Asymmetry Measurements at a Fixed-Target Experiment Using the LHC Proton and Lead Beams (AFTER@LHC),” *Few Body Syst.* **58** no. 4, (2017) 139, [arXiv:1702.01546 \[hep-ex\]](#).
- [32] L. Massacrier, B. Trzeciak, F. Fleuret, C. Hadjidakis, D. Kikola, J. P. Lansberg, and H. S. Shao, “Feasibility studies for quarkonium production at a fixed-target experiment using the LHC proton and lead beams (AFTER@LHC),” *Adv. High Energy Phys.* **2015** (2015) 986348, [arXiv:1504.05145 \[hep-ex\]](#).
- [33] J. P. Lansberg, S. J. Brodsky, F. Fleuret, and C. Hadjidakis, “Quarkonium Physics at a Fixed-Target Experiment using the LHC Beams,” *Few Body Syst.* **53** (2012) 11–25, [arXiv:1204.5793 \[hep-ph\]](#).
- [34] LHCb Collaboration, E. Maurice, “Fixed-target physics at LHCb,” in *5th Large Hadron Collider Physics Conference (LHCP 2017) Shanghai, China, May 15-20, 2017*. 2017. [arXiv:1708.05184 \[hep-ex\]](#). <http://inspirehep.net/record/1616496/files/arXiv:1708.05184.pdf>.
- [35] LHCb Collaboration, L. Anderlini, “Physics programme in fixed-target mode with the LHCb experiment at CERN,” *PoS EPS-HEP2017* (2017) 152.
- [36] S. J. Brodsky and B. T. Chertok, “The Deuteron Form-Factor and the Short Distance Behavior of the Nuclear Force,” *Phys. Rev. Lett.*

- 37 (1976) 269.
- [37] G. Berlad, A. Dar, and G. Eilam, "A Quark-parton Model of Nuclear Production," *Phys. Rev.* **D22** (1980) 1547.
- [38] A. Bodek and J. L. Ritchie, "Fermi Motion Effects in Deep Inelastic Lepton Scattering from Nuclear Targets," *Phys. Rev.* **D23** (1981) 1070.
- [39] A. Bodek and J. L. Ritchie, "Further Studies of Fermi Motion Effects in Lepton Scattering from Nuclear Targets," *Phys. Rev.* **D24** (1981) 1400.
- [40] **European Muon** Collaboration, J. J. Aubert *et al.*, "The ratio of the nucleon structure functions F_{2n} for iron and deuterium," *Phys. Lett.* **123B** (1983) 275–278.
- [41] L. L. Frankfurt and M. I. Strikman, "Hard Nuclear Processes and Microscopic Nuclear Structure," *Phys. Rept.* **160** (1988) 235–427.
- [42] L. W. Whitlow, E. M. Riordan, S. Dasu, S. Rock, and A. Bodek, "Precise measurements of the proton and deuteron structure functions from a global analysis of the SLAC deep inelastic electron scattering cross-sections," *Phys. Lett.* **B282** (1992) 475–482.
- [43] H. Merabet, J. F. Mathiot, J. Dolejsi, and H. J. Pirner, "Modification of the gluon structure function and J/ψ lepton production by nuclear Fermi motion," *Phys. Lett.* **B307** (1993) 177–181.
- [44] S. A. Kulagin, G. Piller, and W. Weise, "Shadowing, binding and off-shell effects in nuclear deep inelastic scattering," *Phys. Rev.* **C50** (1994) 1154–1169, [arXiv:nucl-th/9402015 \[nucl-th\]](#).
- [45] W. Melnitchouk, M. Sargsian, and M. I. Strikman, "Probing the origin of the EMC effect via tagged structure functions of the deuteron," *Z. Phys.* **A359** (1997) 99–109, [arXiv:nucl-th/9609048 \[nucl-th\]](#).
- [46] M. Hirai, S. Kumano, and M. Miyama, "Determination of nuclear parton distributions," *Phys. Rev.* **D64** (2001) 034003, [arXiv:hep-ph/0103208 \[hep-ph\]](#).
- [47] M. M. Sargsian *et al.*, "Hadrons in the nuclear medium," *J. Phys.* **G29** no. 3, (2003) R1–R45, [arXiv:nucl-th/0210025 \[nucl-th\]](#).
- [48] J.-W. Chen and W. Detmold, "Universality of the EMC effect," *Phys. Lett.* **B625** (2005) 165–170, [arXiv:hep-ph/0412119 \[hep-ph\]](#).
- [49] J. Arrington, R. Ent, C. E. Keppel, J. Mammei, and I. Niculescu, "Low Q^2 scaling, duality, and the EMC effect," *Phys. Rev.* **C73** (2006) 035205, [arXiv:nucl-ex/0307012 \[nucl-ex\]](#).
- [50] S. A. Kulagin and R. Petti, "Global study of nuclear structure functions," *Nucl. Phys.* **A765** (2006) 126–187, [arXiv:hep-ph/0412425 \[hep-ph\]](#).
- [51] M. Hirai, S. Kumano, and T. H. Nagai, "Determination of nuclear parton distribution functions and their uncertainties in next-to-leading order," *Phys. Rev.* **C76** (2007) 065207, [arXiv:0709.3038 \[hep-ph\]](#).
- [52] A. Accardi, M. E. Christy, C. E. Keppel, P. Monaghan, W. Melnitchouk, J. G. Morfin, and J. F. Owens, "New parton distributions from large- x and low- Q^2 data," *Phys. Rev.* **D81** (2010) 034016, [arXiv:0911.2254 \[hep-ph\]](#).
- [53] L. B. Weinstein, E. Piasezky, D. W. Higinbotham, J. Gomez, O. Hen, and R. Shneur, "Short Range Correlations and the EMC Effect," *Phys. Rev. Lett.* **106** (2011) 052301, [arXiv:1009.5666 \[hep-ph\]](#).
- [54] A. Accardi, W. Melnitchouk, J. F. Owens, M. E. Christy, C. E. Keppel, L. Zhu, and J. G. Morfin, "Uncertainties in determining parton distributions at large x ," *Phys. Rev.* **D84** (2011) 014008, [arXiv:1102.3686 \[hep-ph\]](#).
- [55] J. J. Ethier and W. Melnitchouk, "Comparative study of nuclear effects in polarized electron scattering from ^3He ," *Phys. Rev.* **C88** no. 5, (2013) 054001, [arXiv:1308.3723 \[nucl-th\]](#).
- [56] P. J. Ehlers, A. Accardi, L. T. Brady, and W. Melnitchouk, "Nuclear effects in the proton-deuteron Drell-Yan process," *Phys. Rev.* **D90** no. 1, (2014) 014010, [arXiv:1405.2039 \[hep-ph\]](#).
- [57] O. Hen, G. A. Miller, E. Piasezky, and L. B. Weinstein, "Nucleon-Nucleon Correlations, Short-lived Excitations, and the Quarks Within," *Rev. Mod. Phys.* **89** no. 4, (2017) 045002, [arXiv:1611.09748 \[nucl-ex\]](#).
- [58] J.-W. Chen, W. Detmold, J. E. Lynn, and A. Schwenk, "Short Range Correlations and the EMC Effect in Effective Field Theory," *Phys. Rev. Lett.* **119** no. 26, (2017) 262502, [arXiv:1607.03065 \[hep-ph\]](#).
- [59] S. I. Alekhin, S. A. Kulagin, and R. Petti, "Nuclear Effects in the Deuteron and Constraints on the d/u Ratio," *Phys. Rev.* **D96** no. 5, (2017) 054005, [arXiv:1704.00204 \[nucl-th\]](#).
- [60] F. Winter, W. Detmold, A. S. Gambhir, K. Orginos, M. J. Savage, P. E. Shanahan, and M. L. Wagman, "First lattice QCD study of the gluonic structure of light nuclei," *Phys. Rev.* **D96** no. 9, (2017) 094512, [arXiv:1709.00395 \[hep-lat\]](#).
- [61] W. Melnitchouk and A. W. Thomas, "Neutron / proton structure function ratio at large x ," *Phys. Lett.* **B377** (1996) 11–17, [arXiv:nucl-th/9602038 \[nucl-th\]](#).
- [62] I. R. Afnan, F. R. P. Bissey, J. Gomez, A. T. Katramatou, W. Melnitchouk, G. G. Petratos, and A. W. Thomas, "Neutron structure function and $A = 3$ mirror nuclei," *Phys. Lett.* **B493** (2000) 36–42, [arXiv:nucl-th/0006003 \[nucl-th\]](#).
- [63] I. R. Afnan, F. R. P. Bissey, J. Gomez, A. T. Katramatou, S. Liuti, W. Melnitchouk, G. G. Petratos, and A. W. Thomas, "Deep inelastic scattering from $A = 3$ nuclei and the neutron structure function," *Phys. Rev.* **C68** (2003) 035201, [arXiv:nucl-th/0306054 \[nucl-th\]](#).
- [64] S. J. Brodsky and G. R. Farrar, "Scaling Laws at Large Transverse Momentum," *Phys. Rev. Lett.* **31** (1973) 1153–1156.
- [65] A. Radyushkin, "Quark Counting Rules: Old and New Approaches," *Int. J. Mod. Phys.* **A25** (2010) 502–512, [arXiv:0907.4585 \[hep-ph\]](#).
- [66] E. Hiyama, Y. Kino, and M. Kamimura, "Gaussian expansion method for few-body systems," *Prog. Part. Nucl. Phys.* **51** (2003) 223–307.
- [67] S. J. Brodsky, H.-C. Pauli, and S. S. Pinsky, "Quantum chromodynamics and other field theories on the light cone," *Phys. Rept.* **301** (1998) 299–486, [arXiv:hep-ph/9705477 \[hep-ph\]](#).
- [68] G. P. Lepage and S. J. Brodsky, "Exclusive Processes in Perturbative Quantum Chromodynamics," *Phys. Rev.* **D22** (1980) 2157.
- [69] S. J. Brodsky and J. R. Primack, "The Electromagnetic Interactions of Composite Systems," *Annals Phys.* **52** (1969) 315–365.
- [70] M. V. Terentev, "On the Structure of Wave Functions of Mesons as Bound States of Relativistic Quarks," *Sov. J. Nucl. Phys.* **24** (1976) 106. [*Yad. Fiz.* 24,207(1976)].
- [71] P. Hoyer and S. Peigne, " J/ψ' to J/ψ ratio in diffractive photoproduction," *Phys. Rev.* **D61** (2000) 031501, [arXiv:hep-ph/9909519 \[hep-ph\]](#).
- [72] J. Hufner, Yu. P. Ivanov, B. Z. Kopeliovich, and A. V. Tarasov, "Photoproduction of charmonia and total charmonium proton cross-sections," *Phys. Rev.* **D62** (2000) 094022, [arXiv:hep-ph/0007111 \[hep-ph\]](#).
- [73] B. Kopeliovich, A. Tarasov, and J. Hufner, "Coherence phenomena in charmonium production off nuclei at the energies of RHIC and LHC," *Nucl. Phys.* **A696** (2001) 669–714, [arXiv:hep-ph/0104256 \[hep-ph\]](#).
- [74] A. Accardi *et al.*, "A Critical Appraisal and Evaluation of Modern PDFs," *Eur. Phys. J.* **C76** no. 8, (2016) 471, [arXiv:1603.08906 \[hep-ph\]](#).
- [75] S. Dulat, T.-J. Hou, J. Gao, M. Guzzi, J. Huston, P. Nadolsky, J. Pumplin, C. Schmidt, D. Stump, and C. P. Yuan, "New parton distribution functions from a global analysis of quantum chromodynamics," *Phys. Rev.* **D93** no. 3, (2016) 033006, [arXiv:1506.07443 \[hep-ph\]](#).
- [76] **NNPDF** Collaboration, R. D. Ball *et al.*, "Parton distributions from high-precision collider data," *Eur. Phys. J.* **C77** no. 10, (2017) 663, [arXiv:1706.00428 \[hep-ph\]](#).
- [77] M. Bonvini, S. Marzani, and C. Muselli, "Towards parton distribution functions with small- x resummation: HELL 2.0," *JHEP* **12** (2017) 117, [arXiv:1708.07510 \[hep-ph\]](#).
- [78] J. Gao, L. Harland-Lang, and J. Rojo, "The Structure of the Proton in the LHC Precision Era," [arXiv:1709.04922 \[hep-ph\]](#).
- [79] H.-W. Lin *et al.*, "Parton distributions and lattice QCD calculations: a community white paper," *Prog. Part. Nucl. Phys.* **100** (2018) 107–160, [arXiv:1711.07916 \[hep-ph\]](#).
- [80] C. Alexandrou, K. Cichy, M. Constantinou, K. Jansen, A. Scapellato, and F. Steffens, "Reconstruction of light-cone parton distribution functions from lattice QCD simulations at the physical point," [arXiv:1803.02685 \[hep-lat\]](#).
- [81] Y.-B. Yang, M. Gong, J. Liang, H.-W. Lin, K.-F. Liu, D. Pefkou,

- and P. Shanahan, “Nonperturbatively-renormalized glue momentum fraction at physical pion mass from Lattice QCD,” [arXiv:1805.00531 \[hep-lat\]](#).
- [82] M. Glueck, E. Reya, and A. Vogt, “Dynamical parton distributions revisited,” *Eur. Phys. J.* **C5** (1998) 461–470, [arXiv:hep-ph/9806404 \[hep-ph\]](#).
- [83] A. S. Rinat and M. F. Taragin, “On distribution functions for partons in nuclei,” *Phys. Rev.* **C72** (2005) 065209, [arXiv:nucl-th/0501006 \[nucl-th\]](#).
- [84] J. Carbonell and V. A. Karmanov, “Relativistic deuteron wave function in the light front dynamics,” *Nucl. Phys.* **A581** (1995) 625–653.
- [85] J. Carbonell, B. Desplanques, V. A. Karmanov, and J. F. Mathiot, “Explicitly covariant light front dynamics and relativistic few body systems,” *Phys. Rept.* **300** (1998) 215–347, [arXiv:nucl-th/9804029 \[nucl-th\]](#).
- [86] A. Accardi, L. T. Brady, W. Melnitchouk, J. F. Owens, and N. Sato, “Constraints on large- x parton distributions from new weak boson production and deep-inelastic scattering data,” *Phys. Rev.* **D93** no. 11, (2016) 114017, [arXiv:1602.03154 \[hep-ph\]](#).
- [87] S. J. Brodsky, J. C. Collins, S. D. Ellis, J. F. Gunion, and A. H. Mueller, “Intrinsic Chevrolets at the SSC,” in *DESIGN AND UTILIZATION OF THE SUPERCONDUCTING SUPER COLLIDER. PROCEEDINGS, 1984 SUMMER STUDY, SNOWMASS, USA, JUNE 23 - JULY 13, 1984*, p. 227. 1984. <http://www-public.slac.stanford.edu/sciDoc/docMeta.aspx?slacPubNumber=SLAC-PUB-15471>.
- [88] M. V. Polyakov, A. Schafer, and O. V. Teryaev, “The Intrinsic charm contribution to the proton spin,” *Phys. Rev.* **D60** (1999) 051502, [arXiv:hep-ph/9812393 \[hep-ph\]](#).
- [89] M. Franz, M. V. Polyakov, and K. Goeke, “Heavy quark mass expansion and intrinsic charm in light hadrons,” *Phys. Rev.* **D62** (2000) 074024, [arXiv:hep-ph/0002240 \[hep-ph\]](#).
- [90] S. J. Brodsky, P. Hoyer, C. Peterson, and N. Sakai, “The Intrinsic Charm of the Proton,” *Phys. Lett.* **93B** (1980) 451–455.
- [91] S. J. Brodsky, C. Peterson, and N. Sakai, “Intrinsic Heavy Quark States,” *Phys. Rev.* **D23** (1981) 2745.
- [92] P. Hoyer and D. P. Roy, “The Intrinsic gluon component of the nucleon,” *Phys. Lett.* **B410** (1997) 63–66, [arXiv:hep-ph/9705273 \[hep-ph\]](#).
- [93] R. Blankenbecler and S. J. Brodsky, “Unified Description of Inclusive and Exclusive Reactions at All Momentum Transfers,” *Phys. Rev.* **D10** (1974) 2973.
- [94] S. J. Brodsky and B. T. Chertok, “The Asymptotic Form-Factors of Hadrons and Nuclei and the Continuity of Particle and Nuclear Dynamics,” *Phys. Rev.* **D14** (1976) 3003–3020.
- [95] S. J. Brodsky, M. Burkardt, and I. Schmidt, “Perturbative QCD constraints on the shape of polarized quark and gluon distributions,” *Nucl. Phys.* **B441** (1995) 197–214, [arXiv:hep-ph/9401328 \[hep-ph\]](#).